Equivalent load profile development for fatigue testing of a 13 meter wind turbine blade

Afrooz Kazemi Vanhari[1,2], Edward Fagan[1,2], Yadong Jiang[1,2], Patrick Meier[1,2], William Finnegan[1,2], Jamie Goggins[1,2]
[1]Civil Engineering, School of Engineering, College of Science & Engineering, National University of Ireland Galway, University Road, Galway, Ireland, H91 TK33
[2]SFI MaREI Research Centre for Energy, Climate and Marine, Ryan Institute, National University of Ireland Galway, University Road, Galway, Ireland, H91 TK33
email: afrooz.kazemi@nuigalway.ie, edward.fagan@nuigalway.ie, yadong.jiang@nuigalway.ie, patrick.meier@nuigalway.ie, william.finnegan@nuigalway.ie, jamie.goggins@nuigalway.ie

ABSTRACT: Since one of the most common problems with wind turbine blades is fatigue failure, full-scale fatigue testing is an effective way to validate the performance of a wind turbine blade. In this paper, the fatigue test loads in both edgewise and flatwise directions for a 13 metre wind turbine blade are derived, and used to determine an equivalent design life loading to apply in a full-scale fatigue test in the Large Structures Research Laboratory (LSRL) located in the Alice Perry Engineering Building, NUI Galway. The blade is constructed from glass-fibre reinforced powder epoxy composite material and consists of two internal shear webs. The blade is supported at its root on a frame constructed from S355 grade steel, and three hydraulic actuators (capacities range from 250 kN to 750 kN) work in concert to apply the flatwise and edgewise bending moment distribution along the blade. To develop the fatigue test load, aeroelastic simulation tools, including AeroDyn and FAST, are used to obtain the load time series under power producing, starting, stopping, and parking situations according to the International Electrotechnical Commission 61400-1 standard. The Rainflow counting method is used to extract the number of cycles for combinations of stress range and mean stress from the input load series. The Goodman method is employed for computing the number of permissible cycles for each combination of stress range and mean values and the Palmgren–Miner rule is applied for the cumulative damage calculation. For the operational load cases analysed, it was found that there was a negligible risk of fatigue damage for the unidirectional materials in the blade. The areas of the blade that showed a higher risk of fatigue were plies near the root of the blade, at the leading and trailing edges; however, the expected lifetime still exceeded the 20 year design life of the blade.

KEYWORDS: Wind turbine blade; Full-scale fatigue test; Goodman method; Palmgren–Miner rule; Fatigue damage; Fatigue lifetime.

1 INTRODUCTION

Over the last few years, the wind turbine market is growing rapidly and becoming more and more competitive. The blade, as a critical component of the wind turbine system, must be capable of surviving for more than 20 years according to the International Electrotechnical Commission (IEC) 61400-1 standard and the Germanischer-Lloyd (GL) regulations [1][2]. During the life span, the blades can be damaged after hundreds of millions of fatigue load cycles, which are much higher than that experienced by a bicycle, car, helicopter blades, and bridge [3]. From the fatigue point of view, only three load components are the main drivers for the fatigue damage; namely the axial force and the flatwise and edgewise bending moment time histories [4]. Among these loads, edgewise bending moments and flatwise bending moments typically cause approximately 97% of the fatigue damage in the blade [5].

Thus, this study describes a methodology to estimate the fatigue damage for the unidirectional materials (UD), and to derive the equivalent fatigue test loads of a 13 m wind turbine blade in both flatwise and edgewise directions due to the bending moments. This 13 m blade is constructed of glass-fibre reinforced powder epoxy composite and consists of two internal shear webs. In this paper, after defining a turbine geometry for the 13 m blade according to its length, the loads are calculated using FAST [13] under power producing, starting, stopping, and parking situations. The Palmgren–Miner (PM) rule is used for cumulative damage calculation. The Goodman method is used for computing the allowed load cycle number, and the Rainflow method is employed to determine the number of events with a given combination of mean stress and stress range. Figure 1 shows this 13 m wind turbine blade in the Large Structure Research Laboratory (LSRL) located in the Alice Perry Engineering Building, NUI Galway, which is supported at the root by a support frame made of S355 grade steel.

Figure 1. The 13 m blade at LSRL

2 METHODS

2.1 Turbine data for the 13 m blade

To find the best turbine that can be installed with the 13 m blade, existing turbines (nearly 130 turbines) with a rotor diameter between 25 and 31 meters were found from [6]. Examining turbine parameters such as the number of blades, hub radius, hub height, etc., helped the authors find the best turbine that can be attached to the 13 m blade. Among these parameters, the hub height could play an important role in the

choice of turbine [7]. Thus, based on the existing turbine data (Figure 2), United States Geological Survey (USGS) dataset [8] and the wind turbines installed in the Netherlands [9], it was concluded that a turbine with a hub height between 30 and 45 m can be an optimal choice for the 13 m blade. Therefore, among the existing turbines from [6], depending on the hub height between 30 and 45 m, the AWT27 was selected for the 13 m blade since all the information about this turbine as an example test of FAST [13], is also available. Therefore, a three-bladed AWT27 turbine attached to the 13 m blade was analysed in this paper.

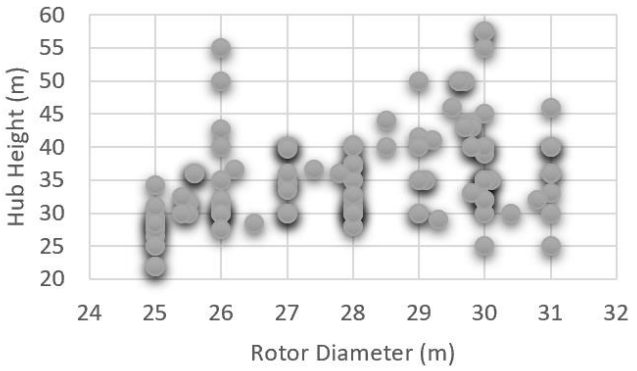

Figure 2. Wind turbines database from [6], hub height versus rotor diameter

2.2 Calculating the loading

In this part, NuMAD [10], PreComp [11], ModeShape, JavaFoil, AeroDyn [12], and FAST [13] were used to obtain the dynamic and structural response of the 13 m blade, including edgewise bending moment and flatwise bending moment for 10 minute intervals under different load cases, such as power producing, starting, stopping, and parking.

Using AeroDyn, the initial conditions required for FAST, including rotor speed and pitch angle, were found for each wind speed, with the fact that the wind turbine starts to operate when the wind speed is greater than the cut-in speed. The rotation speed of the rotor increases with increasing wind speed until rated speed. When the wind speed is above the rated speed, the pitch control system will adjust the blade pitch angle, and the wind turbine stalls when the wind speed is beyond the cut-out speed. Figures 3 and 4 show the calculated initial conditions for FAST and the power for the selected turbine, respectively. Note that since the 13 m blade installation is 3.3 degrees at the LSRL, this angle is used as the initial blade pitch for wind speed between cut-in and rated in the analysis.

According to the available data from [6] in Figure 5, the rated power of 200-300 KW is the most common power for this range of blade lengths that can confirm that the power of 300 kW is a qualified choice for the selected turbine.

Finally, Figure 6 shows the edgewise and flatwise bending moment in power producing situations at node 0.72 m for a wind speed of 8.5 m/s.

Given that the three most important sources of the loading of a wind turbine are gravitational loading, inertial loading, and aerodynamic loading, the gravitational effect is seen at the edgewise bending moment as a dominant sinusoidal variation, on which some small high frequency signal is located due to the atmospheric turbulence. However, the flatwise bending moment is greatly affected by the aerodynamic loads that vary with the turbulent wind field and, therefore, this signal is more random.

In addition, the frequency of the sinusoidal loading of the blades depends on the rotation of the rotor, which is often determined by 1π. For example, the rotor speed of the blade in Figure 6 is 27 rpm or 2.8 rad/s and the sinusoidal load frequency is approximately 1.3 rad/s, which is close to 1π (1.4 rad/s).

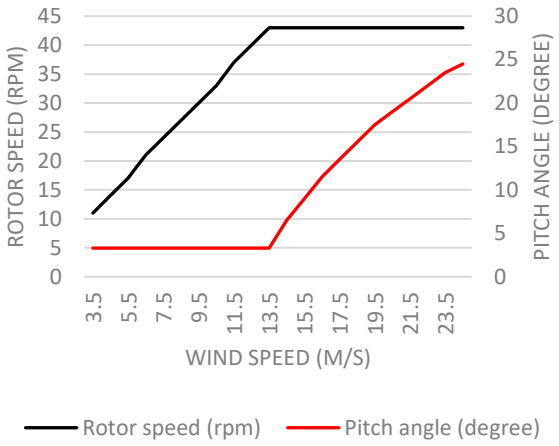

Figure 3. Initial conditions for the selected turbine

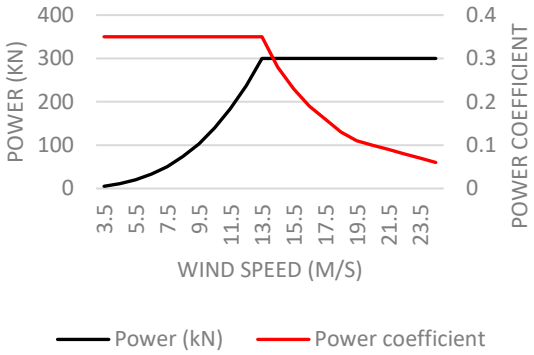

Figure 4. Power and power coefficient for the selected turbine

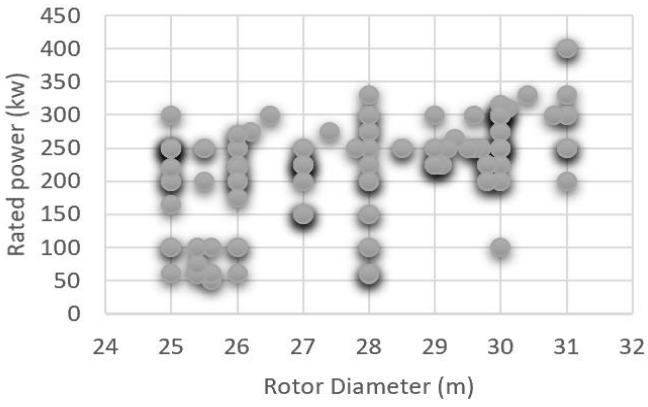

Figure 5. Wind turbine database from [6], rated power versus rotor diameter

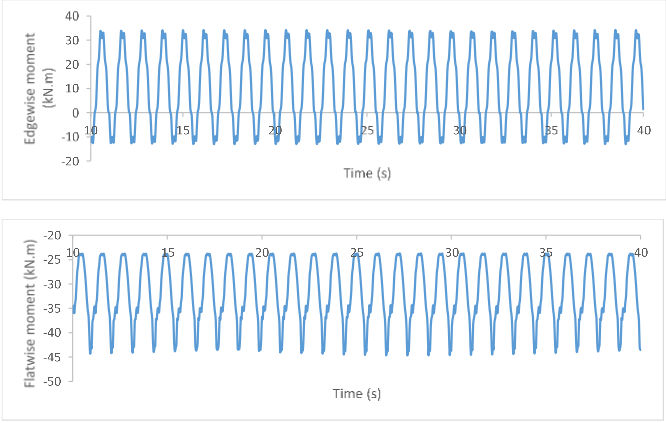

Figure 6. Bending moment calculated from FAST

2.3 *Rainflow counting and Markov matrix*

For each 10 minutes time history, the bending stresses are sorted in a matrix, where the elements denote the number of cycles due to the mean bending stress and range bending stress for each wind speed. To count the number of cycles from an actual time series, a technique called 'Rainflow counting' is used. Thus, a software program was created in MATLAB to extract Rainflow cycles from each 10 minutes time history. Figure 7 shows the Rainflow counting in power producing situations at node 0.72 m with the wind speed of 8.5 m/s.

The Rainflow shows that for these power producing situations, the small moment ranges up to 6 kNm, which are due to the atmospheric turbulence, are more in number, and contribute more to the fatigue failure than the large stress ranges.

After performing the Rainflow counting, knowing the annual wind distribution, the probability, *f*, of the wind speed is computed because the actual number of annual 10 minute periods is 6×8760×f. Typically, the probability density function of the wind is given by either a Rayleigh or a Weibull distribution. As shown in Figure 8, the Rayleigh distribution according to Equation 1 is used in this paper.

$$P_R(V_{hub}) = 1 - \exp\left[-\pi\left(V_{hub}/2V_{ave}\right)^2\right] \quad (1)$$

where, in the standard wind turbine classes, V_{ave} shall be chosen as $0.2V_{ref}$ [1].

The number of cycles per year, *n*, in the mean and range stress is found by adding together the contributions from each wind speed interval. The matrix, with elements n_{ij}, is called the Markov matrix. All the loads from power producing, startup, normal shut down, and parked should be added to the Markov matrix. To create this matrix, the MATLAB implementation is used.

2.4 *Fatigue damage*

Fatigue damage is measured by a metric such as the cumulative damage *D* in the Palmgren–Miner (PM) rule, which the criteria for not failing is that D is less than 1.

$$\sum \frac{n}{N} = D < 1 \quad (2)$$

where n is the number of load cycles for a given stress amplitude/mean combination due to the Markov matrix and N is the number of permissible load cycles for a given stress amplitude/mean combination.

In order to calculate the permissible number of cycles for a given stress state, based on the Goodman method, the following formula was used [2]:

$$N = \left[\frac{R_{k,t} + |R_{k,c}| - |2 \cdot \gamma_{Ma} \cdot S_{k,M} - R_{k,t} + |R_{k,c}||}{2 \cdot (\gamma_{Mb}/C_{1b}) \cdot S_{k,A}}\right]^m \quad (3)$$

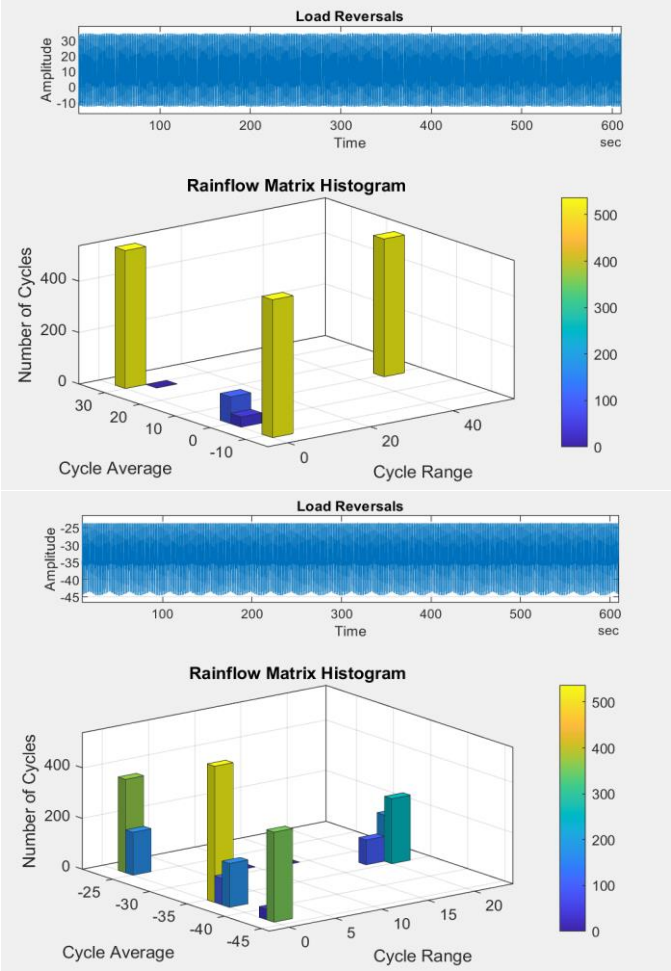

Figure 7. Rainflow counting, the top figure for edgewise bending moment and the bottom figure for flatwise bending moment

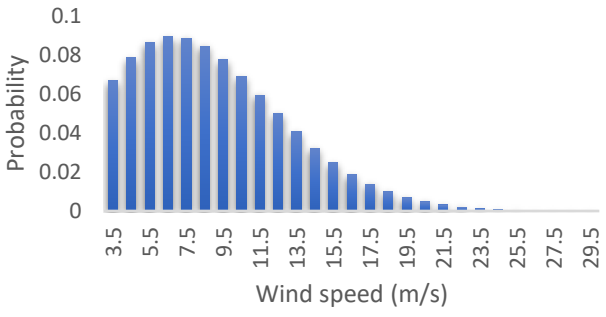

Figure 8. Rayleigh wind speed distribution

where $R_{k,t}$ is the maximum tensile strain (Micro strain), $R_{k,c}$ is the maximum compression strain (Micro strain), m is the slope of the S−N diagram (for simplified assumptions is equal to 10 for laminates with epoxy resin matrix), $\gamma_{Ma,\,Mb}$ are the safety factors, $S_{k,M}$ is the mean strain due to the Markov matrix and $S_{k,A}$ is the amplitude strain due to the Markov matrix.

The safety factors are calculated according to:

$$\gamma_{Mx} = \gamma_{M0} \prod_i C_{ix} \tag{4}$$

where γ_{M0} = 1.35, and the values assigned to C_{ix} are selected according to the material used in the blade manufacturing (Table 1).

Table 1. Values of safety factors

C_{ix}	Description	Value
C_{1a}	Influence of aging	1.35
C_{2a}	Temperature effect	1.1
C_{3a}	Laminate production	1.1
C_{4a}	Post-cured laminate	1
C_{1b}	Temperature effect	1.1
C_{2b}	UD reinforcement products	1
C_{3b}	Post-cured laminate	1

To find $S_{k,M}$ and $S_{k,A}$, since the data in the Markov matrix is bending moments with the unit of kNm, a transfer function (strain/bending moment) is needed to convert the bending moments (kNm) to strain. According to well-known equations of $\sigma = My/I$ and $\varepsilon = \sigma/E$, the transfer function ε/M is equal to the y/EI, where σ is the bending stress, M is the bending moment, Y is the vertical distance away from the neutral axis, ε is the strain, and E is the modulus of elasticity.

Thus, it can be concluded that the transfer function is independent of the type of load, but dependent on the shape of the structure (y, E, I). Therefore, with an optional loading in appropriate direction, the transfer function (ε/M) can be found for each point. By multiplying the transfer function to the bending moment of the same point, the strain of that point can be obtained. In this study, the transfer function is found from Abaqus by applying 1 kN load at the tip that causes the root bending moment of 12.96 KNm. Since the aerodynamic torque loads generate tensile and compressive sides in the flatwise direction, and the aerodynamic thrust loads generate tensile and compressive stress along the blade leading and trailing in the edgewise direction, there are four types of transfer functions for UD materials, two for the tensile and compressive sides in the flatwise direction and the other two for along the blade leading and trailing in the edgewise direction. Note that the UD material has been studied because it is the most worrying part of the blade due to fatigue damage caused by bending moments.

After finding the transfer functions, the number of tolerable load cycles (N) with a given mean and range stress (regarding Markov matrix) can be achieved at each node. Figure 9 is an example of the permissible load cycle at node 0.72 m for the tensile side. As can be seen from Figure 9, the effect of mean strain on finding the number of cycles is not appreciable. For this reason, sometimes only the range is taken into account and the influence of the mean stress level is ignored. However, this study included the effect of the mean strain.

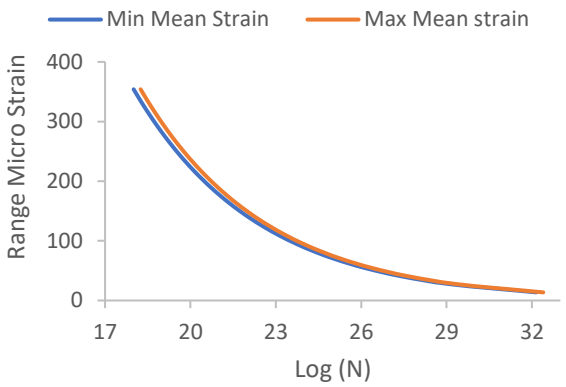

Figure 9. Permissible load cycle

By finding N, lifetime and fatigue damage for 20 years can be estimated at each node for both directions. Based on the estimating figures (Figures 10 and 11), the highest fatigue damage appears near the root on the trailing and leading edge due to the edgewise bending moment, in which fatigue damage of the trailing edge is more than the leading edge. The reason for this could be the gravity load that affects the leading and trailing edges of the blade and since the vertical distance from the neutral axis of the trailing edge is more than leading-edge, the fatigue damage appears more in the trailing edge. In addition, it can be concluded that the fatigue damage of the compression side is more than the tensile side, since composite materials have lower compressive strength than tensile strength. However, the blade is safe because the computed fatigue life values are higher than the required design life of 20 years.

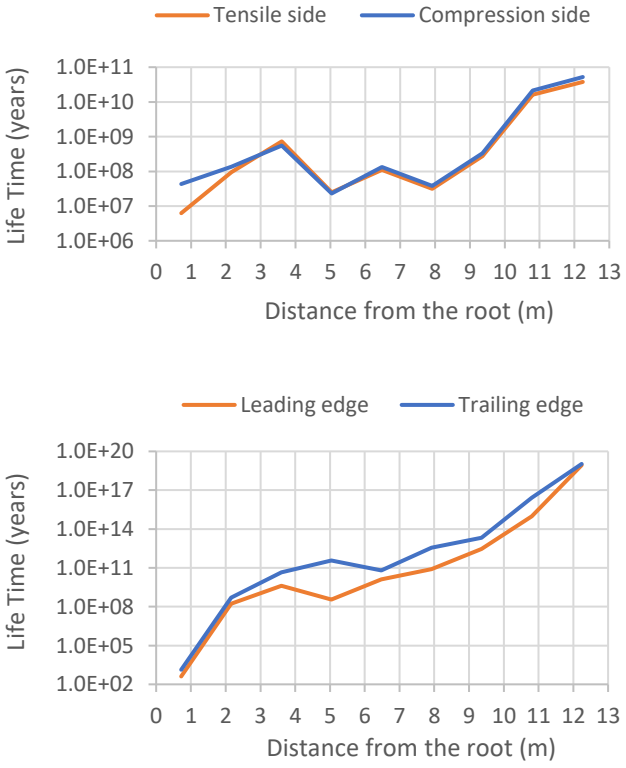

Figure 10. Lifetime along the blade

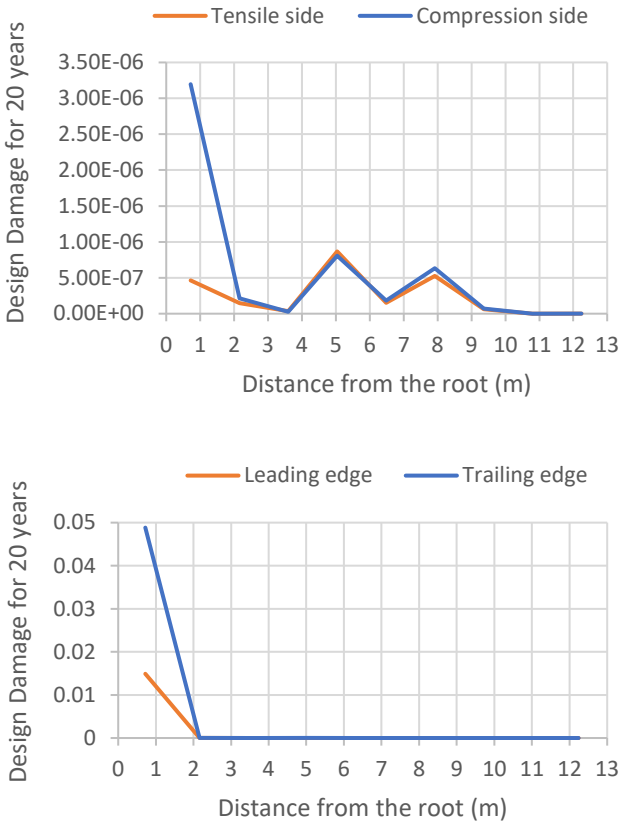

Figure 11. Design damage for 20 years along the blade

2.5 Equivalent bending moment

To compare the contribution from the different wind speeds to the total fatigue damage, an equivalent load can be used. The equivalent load is defined as the cyclic load which, when applied equivalent *n* times, gives the same fatigue damage on the wind turbine as the real turbulent flow at the considered wind speed. The equivalent number of cycles is dependent on the number of days of the test and the frequency of the loading defined by the actuator [14]. The test is considered to be performed in 45 days (8 hours) with a frequency of 0.1 Hz. Thus, the number of cycles will be 129,600.

It is worth noting that the R-value for loading was considered as 0.1.

Since the test damage should be equal to the obtained design damage, the equivalent mean and range load can be calculated for the tensile side. For the compressive side, as the load cannot be applied separately, the equivalent load defined by the tensile analysis is applied for this side. As a result, only the number of test days for this side should be different from the tensile side.

The same procedure is used for flatwise bending moment. Tables 2 and 3, as well as Figures 12 and 13, show the equivalent fatigue test loads for both directions in kNm.

The developed bending moments will be applied to the blade in the Large Structure Research Laboratory (LSRL) located in the Alice Perry Engineering Building, NUI Galway. The results will be validated with the FE models and predictions in this study.

Table 2. Equivalent edgewise bending moment in kNm

Location (m)	Mean (kNm)	Range (kNm)	Max (kNm)	Min (kNm)
0.72	82.5	135.1	150.1	15.0
2.16	53.0	86.7	96.4	9.6
3.6	37.0	60.6	67.4	6.7
5.04	24.4	40.0	44.4	4.4
6.48	14.7	24.0	26.7	2.7
7.92	8.0	13.0	14.5	1.5
9.36	3.6	5.8	6.5	0.7
10.8	1.0	1.6	1.8	0.2
12.24	0.1	0.2	0.2	0.0

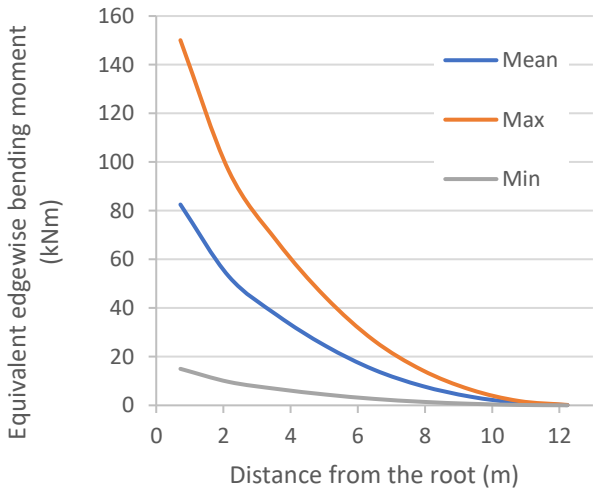

Figure 12. Equivalent edgewise bending moments

Table 3. Equivalent flatwise bending moments in kNm

Location (m)	Mean (kNm)	Range (kNm)	Max (kNm)	Min (kNm)
0.72	49.1	80.4	89.4	8.9
2.16	36.3	59.4	66.0	6.6
3.6	26.1	42.6	47.4	4.7
5.04	19.2	31.4	34.9	3.5
6.48	13.0	21.2	23.6	2.4
7.92	8.4	13.7	15.2	1.5
9.36	4.3	7.1	7.9	0.8
10.8	1.6	2.6	2.8	0.3
12.24	0.2	0.3	0.4	0.0

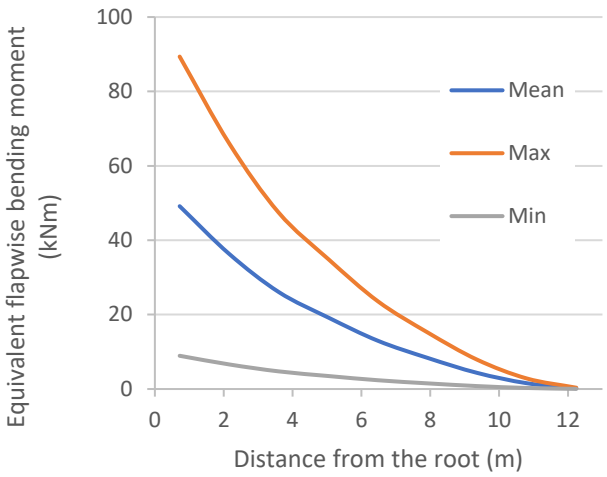

Figure 13. Equivalent flatwise bending moments

3 CONCLUSIONS

In this paper, a method for converting the load spectrum of a 13 m wind turbine blade into the test load for a full-scale fatigue test is presented. The fatigue loads are computed from FAST for DLC 1.2, 3.1, 4.1, 6.4 referring to the power producing, starting, stopping, and parking situations, respectively, according to the IEC 61400-1 standard. The fatigue damage prediction is carried out using the fatigue damage modelling approach recommended by DNV GL (using the Goodman method). Based on this study, the blade experiences a fatigue gravity load of over 283 million cycles. Thus, the stresses from the gravity loading are an important consideration in the fatigue analysis. In addition, the present study suggests that the mean-stress effect may be ignored by simply performing a fatigue life study based on the Goodman equation. Under this assumption, the S-N curve, which is a power law function, consisting of the ratio of the local stress range to the material strength all to the power of a material constant that is equal to 10 for laminates with epoxy resin matrix according to [10].

For the operational load cases analysed, it was found that there was negligible risk of fatigue damage for the unidirectional materials in the blade. The areas of the blade that showed a higher risk of fatigue were plies near the root of the blade, at the leading and trailing edges; however, the expected lifetime exceeded the 20 year design life of the blade. Finally, the developed bending moments will be applied to the blade in the Large Structure Research Laboratory (LSRL) located in the Alice Perry Engineering Building, NUI Galway. The results will be validated with the FE models and predictions in this study.

ACKNOWLEDGMENTS

The authors would like to acknowledge the support from Science Foundation Ireland (SFI) through the SFI MaREI Research Centre for Energy, Climate and Marine (Grant no.: 12/RC/2302_2) and from the European Commission, through the Executive Agency for Small and Medium sized Enter-prises (EASME) under the LEAPWind project (Agreement no.: EASME/EMFF/2017/1.2.1.12/S1/06/SI2.789307) and through MaRINET2 (grant agreement no.: 26255). Additional thanks are given to the technical staff at the Large Structures Research Laboratory, NUI Galway.

REFERENCES

[1] IEC, “International standard IEC 61400-1, Wind turbines Part 1: Design requirements,” *Int. Stand.*, vol. 2005, 2005.
[2] G. L. Wind, “Chapter 1 General Conditions for Approval,” 2010.
[3] L. Mishnaevsky, K. Branner, H. N. Petersen, J. Beauson, M. McGugan, and B. F. Sørensen, “Materials for wind turbine blades: an overview,” *Materials (Basel).*, vol. 10, no. 11, p. 1285, 2017.
[4] K. Hayat, M. Asif, H. T. Ali, H. Ijaz, and G. Mustafa, “Fatigue life estimation of large-scale composite wind turbine blades,” *Proc. 2015 12th Int. Bhurban Conf. Appl. Sci. Technol. IBCAST 2015*, pp. 60–66, 2015.
[5] M. Sathyajith and G. S. Philip, *Advances in wind energy conversion technology*. Springer Science & Business Media, 2011.
[6] “Wind turbines database | list.” [Online]. Available: https://en.wind-turbine-models.com/turbines?view=table. [Accessed: 05-May-2020].
[7] R. Wass, “Design of Wind Turbine tower Height and Blade Length: an Optimization Approach,” p. 72, 2018.
[8] J. E. Diffendorfer, L. A. Kramer, Z. H. Ancona, and C. P. Garrity, “Onshore industrial wind turbine locations for the United States up to March 2014,” *Sci. data*, vol. 2, no. 1, pp. 1–8, 2015.
[9] W. G. J. H. M. Van Sark, H. C. Van der Velde, J. P. Coelingh, and W. A. A. M. Bierbooms, “Do we really need rotor equivalent wind speed?,” *Wind Energy*, vol. 22, no. 6, pp. 745–763, 2019.
[10] J. Berg and B. Resor, “Numerical manufacturing and design tool (NuMAD V2. 0) for wind turbine blades: User’s guide,” *Sandia Natl. Lab. Albuquerque, NM, Tech. Rep. No. SAND2012-728*, no. August, 2012.
[11] G. Bir, “User’s Guide to PreComp (Pre-Processor for Computing Composite Blade Properties),” *Natl. Renew. Energy Lab.*, no. September, p. 31, 2005.
[12] J. M. Jonkman, G. J. Hayman, B. J. Jonkman, and R. R. Damiani, “AeroDyn v15 User’s Guide and Theory Manual,” *Renew. Energy*, no. March, p. 46, 2015.0
[13] J. M. Jonkman and M. L. B. Jr, “FAST User ’ s Guide,” *Natl. Renew. Energy Lab.*, 2005.
[14] M. O. L. Hansen, *Aerodynamic of Wind Turbines*. 2008.